Supporting information

Synthesis and Charge-Transporting Properties of Electron-Deficient CN_2-Fluorene Based D-A Copolymers

Jianhua Huang [a,e], Yan Zhao [b], Xunlei Ding [c], Hui Jia [a], Bo Jiang [a], Zhiguo Zhang [b], Chuanlang Zhan *[,a], Shenggui He [c], Qibing Pei *[,d], Yongfang Li [b], Yunqi Liu [b], Jiannian Yao *[,a]

1. Materials and methods.

The ^{1}H NMR and ^{13}C NMR spectra were measured on a Bruker AVANCE 400 MHz spectrometer using tetramethylsilane (TMS; δ = 0 ppm) as an internal standard. Mass spectrum (MALDI-TOF-MS) was determined on a Bruker BIFLEX III mass spectrometer. Elemental analysis was performed on a flash EA1112 analyzer. IR spectra were recorded on a TENSOR-27 spectrometer using KBr pellets. The molecular weight of the copolymers was measured by gel permeation chromatograph (GPC) in THF using polystyrene as a standard. Thermogravimetric analysis (TGA) was performed on a Perkin-Elmer TGA-7 at a heating rate of 10℃/min under nitrogen flow. UV-vis absorption spectrum was recorded on a Hitachi U-3010 spectrometer. The electrochemical measurements were carried out in a deoxygenated solution of tetra-n-butylammonium hexafluorophosphate (Bu_4NBF_6, 0.1 M) in acetonitrile with a computer-controlled Zennium electrochemical workstation. A glassy carbon electrode, a Pt wire, and an Ag/AgCl electrode were used as the working, counter, and reference electrodes, respectively. Copolymer thin films for X-ray diffraction (XRD) were prepared by drop-casting of chloroform solutions on silica slides. The XRD pattern was recorded by a Rigaku D/max-2500 diffractometer operated at 40 kV voltage and a 200 mA current with Cu Kα radiation.

All of the starting materials and solvents for organic synthesis were purchased from Sigma Aldrich, Alfa Aesar, or Beijing Chemical Works and were used without further purification, unless otherwise stated. THF and toluene were distilled from sodium benzophenone under nitrogen before use. Cyclic voltammetry test of $PC_{61}BM$ was measured on a computer-controlled Zennium electrochemical workstation, in a 0.1 mol/L tetrabutylammonium hexafluorophosphate chlorobenzene/acetonitrile (5:1) solution, with a glassy carbon electrode, a Pt wire, and an Ag/AgCl electrode as the working, counter, and reference electrodes, respectively.

2. DFT calculations

Density functional theory (DFT) calculations were performed using the Gaussian 03 program[1] with the B3LYP exchange-correlation functional.[2-4] All-electron triple-ξ valence basis sets with polarization functions (6-311G**) are used for all atoms. Geometry optimizations were performed with full relaxation of all atoms. For each molecule, various conformations with different dihedral angles were optimized, and the data for the one with the lowest energy are reported. Vibrational frequency calculations were performed to check that the stable structures have no imaginary frequency. The electronic excitation energies and oscillator strengths were computed with time-dependent DFT (TD-DFT)[5] to simulate the UV-Vis spectra (half-width at half height was set to 0.1 eV).

3. Fabrications and Characterizations of the OTFTs.

An n-type heavily doped Si wafer with a SiO_2 layer of 300 nm (with a capacitance of 11 nF·cm^{-2}) served as the bottom gate electrode and dielectric layer, respectively. The bottom Au contacts were prepared by photolithography and the device channel lengths, defined as the distance between source and drain was 5 μm. The channel width was 1400 μm. Before deposition of the organic semiconductor, the gate dielectrics were treated with octadecyltrichlorosilane (OTS) in a vacuum oven at a temperature of 120°C, forming an OTS self-assembled monolayer. The treated substrates were rinsed successively with heptane, ethanol, and chloroform. A copolymer layer was deposited on the OTS-treated Si/SiO_2 substrates by spin-coating a chlorobenzene (CB) solution (10 mg/mL) of **P1**, **P2**, **P3**, or **P4**. The resulting thin film was annealed at 80°C for 60 minutes in vacuum to remove the solvent and improve the film quality and morphology. The field-effect mobility was calculated in the saturation region using the following equation: $I_{ds}=(WC_i/2L)\mu(V_G-V_T)^2$, where I_{ds} is the drain-source current, W and L are the channel width (1400 μm) and length (5 μm), respectively, μ is the field-effect mobility, C_i is the capacitance per unit area of the insulation layer (SiO_2, 11 nF·cm^{-2}), V_T and V_G are the gate and threshold voltages, respectively.

4. Fabrications and Characterizations of the OSCs.

The OSCs were fabricated with configurations of ITO/PEDOT: PSS/**P3**: $PC_{61}BM$/Ca/Al. The indium tin oxide (ITO) glass was pre-cleaned, respectively, with deionized water, acetone, and isopropanol and treated in an ultraviolet-ozone chamber (Jelight Company) for 30 min. A thin layer (30 nm) of poly(3,4-ethylene-dioxythiophene):poly(styrenesulfonate) (PEDOT:PSS, Baytron PVPAI 4083, Germany) was spin-coated onto the pre-cleaned ITO glass and baked at 120℃ for 1 hour. A 1,2-dichlorobenzene solution of **P3**/$PC_{61}BM$ (40 mg/mL, 1:1, w/w) was subsequently spin-coated on the surface of the PEDOT:PSS layer to form a photoactive layer. The film thickness of the photoactive layer is about 50nm. Then, the Ca(20 nm)/Al(80 nm) cathode was deposited on the photoactive layer by vacuum evaporation. The effective area of OSCs is 4 mm^2. The current-voltage (*I-V*) curves of the OSCs were measured on a computer-controlled Keithley 236 Source Measure Unit. A xenon lamp with AM1.5 filter was used as the white light source, and the optical power on surface of the OSCs was 100 mW/cm^2.

4. Supporting Figures

Figure S1. (a) X-ray diffraction (XRD) patterns of the copolymer thin films. (b) Amplified graphic of (a) from 2θ = 10° to 30°, which is the weak π-π stacking pattern of the polymer chains. The weak and broad reflections around 2θ = 20°—25° are corresponding to a *d*-spacing ranging from 4.0 Å—3.6 Å, consistent with the normal and amorphous π-π stacking distance observed from the polymer films.[6] Although the four copolymers exhibited weak π-π stacking patterns, **P3** exhibits well-defined (100) and (200) reflections, indicating its relatively ordered and compact lamellar structure in films.

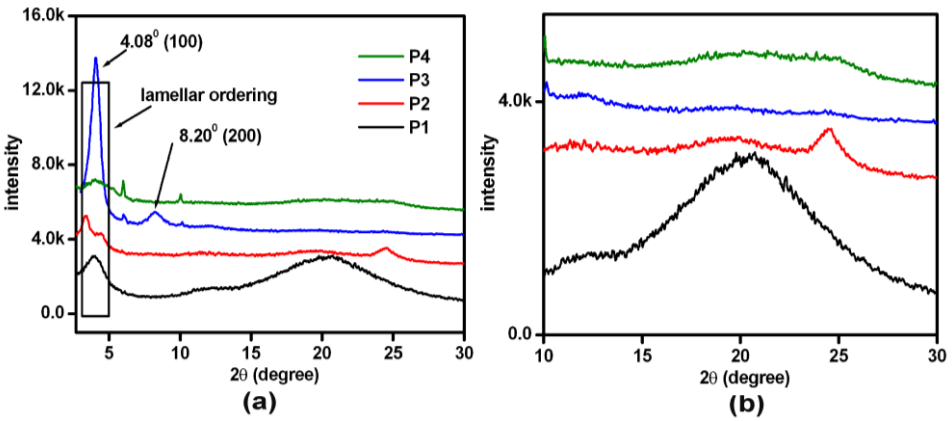

Figure S2. Schematic diagram of hybridizations between the donor (D) and acceptor (A). (The colors symbolically represent the participation rates of energy levels of D and A in the hybridization).

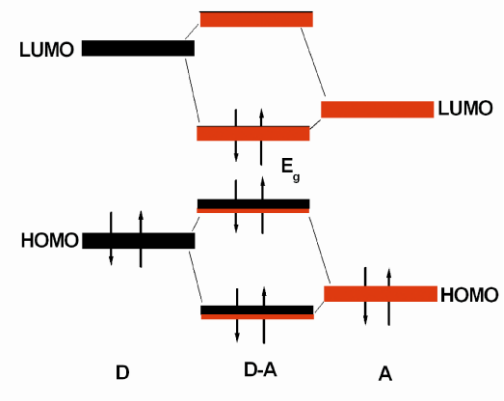

Figure S3. HOMO and LUMO surface plots of the four donor units of 9-alkylfluorene (AF, a), benzodithiophene (BDT, b), bithiophene (BT, c), and dithienopyrrole (DTP, d) and CN_2-Fluorene acceptor unit (e).

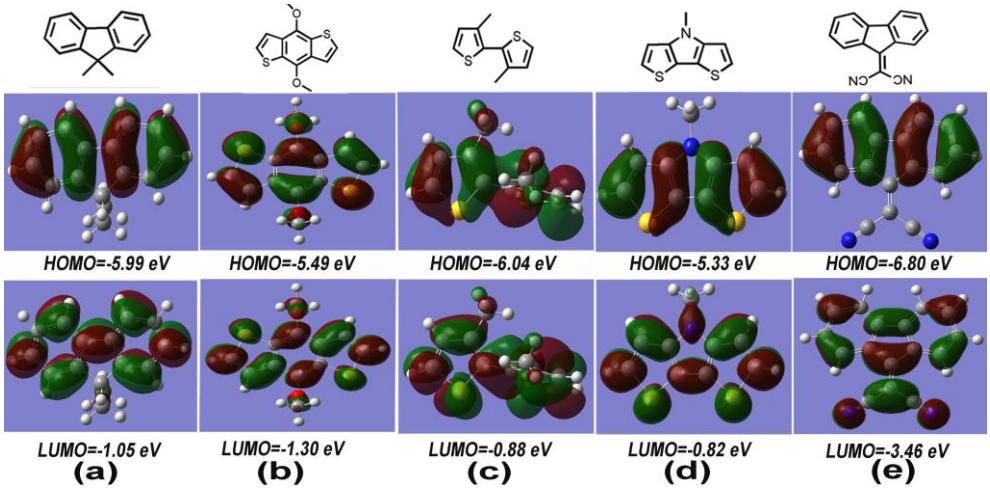

Figure S4. Calculated absorption spectra of the polymers of **P1**, **P2**, **P3** and **P4**.

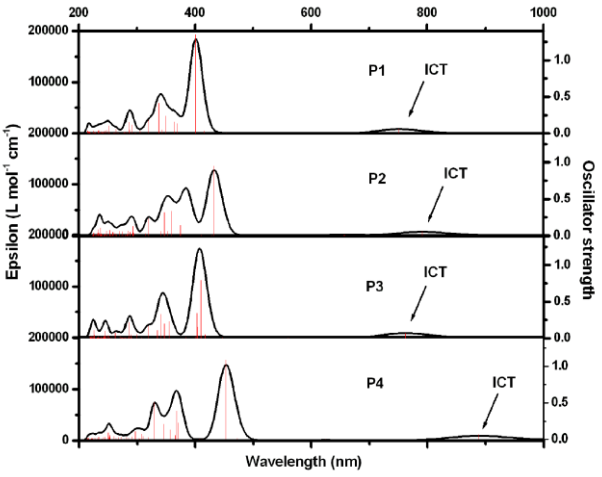

Figure S5. Franck-Condon principle diagram. The red color represents the two vibrational wavefunctions overlap of HOMO (S_0) and LUMO (S_n). We attribute the weak ICT transitions (HOMO-LUMO transitions) of the four copolymers to the little overlap between the HOMO wave functions and LUMO wave functions.

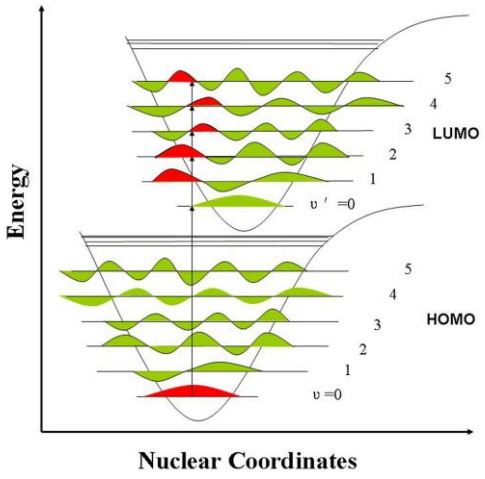

Figure S6. Current density-voltage (*I-V*) characteristics of OSCs with a structure of ITO/PEDOT:PSS/**P2**:$PC_{61}BM$ (1:1, w/w)/Ca/Al (left) and ITO/PEDOT:PSS/**P3**:$PC_{61}BM$ (1:1, w/w)/Ca/Al (right).

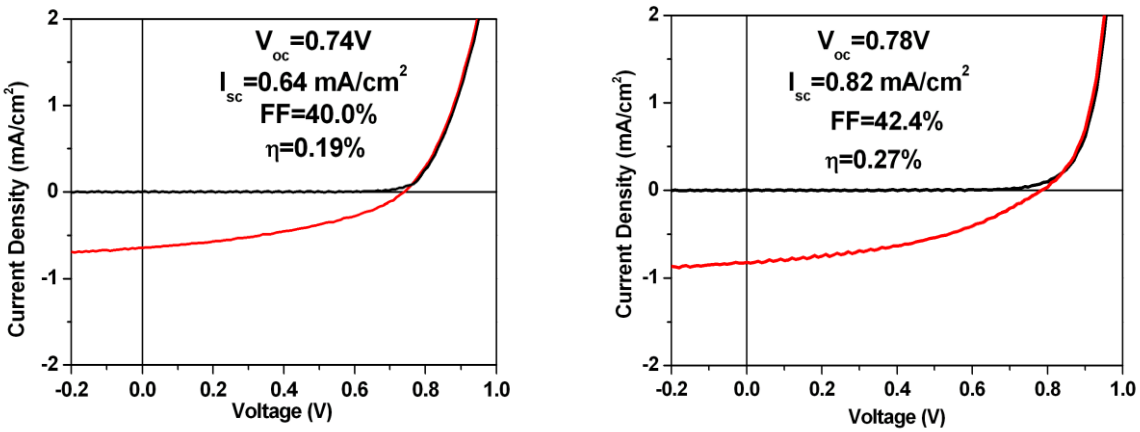

Figure S7. Cyclic voltammograms of **$PC_{61}BM$** in chlorobenzene/acetonitrile (5:1) solution with 0.1M Bu_4NBF_6 at 100mV/s, which was measured using the computer-controlled Zennium electrochemical workstation, the instrument using for determinations of the redox properties of the copolymers of **P1**, **P2**, **P3**, and **P4**.

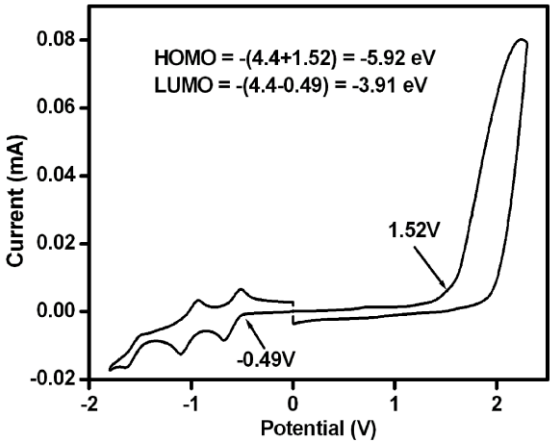

5. Supporting Tables

Table S1. Optical and electrochemical properties of the copolymers of **P1**, **P2**, **P3**, and **P4**.

Copolymer	λ^a_{max}(nm)[a] solution	λ^a_{max}(nm)[a] film	$\Delta\lambda^a_{max}$ (nm)	A_{ICT}/A_{donor}[c] (solution/solid)	λ_{onset}(nm)[b] /E_g^{opt} (eV)[d]	E_{ox}^{onset}(V)[e] /HOMO (eV)[f]	E_{red}^{onset} (V)[e] /LUMO (eV)[f]	E_g^{cv} (eV)[g]
P1	400, 490	414, 496	14/6	0.14/0.25	670/1.85	1.21/–5.61	–0.83/–3.57	2.04
P2	464, 665	470, 667	6/2	0.08/0.13	893/1.39	0.79/–5.19	–0.77/–3.63	1.56
P3	446, 692	463, 727	17/35	0.06/0.11	939/1.32	0.68/–5.08	–0.60/–3.80	1.28
P4	453, 701	505, 733	52/32	0.05/0.09	971/1.28	0.45/–4.85	–0.73/–3.67	1.18

[a] Absorption maxima. [b] The onset edge of absorption in the copolymer film. [c] The A_{ICT}/A_{donor} was defined as the ratio of the maximum absorbance of the 600–1000 nm ICT band (A_{ICT}) versus the maximum absorbance of the 350–600 nm band from the conjugate donor units (A_{donor}). [d] Optical bandgap estimated from the onset edge of absorption in the copolymer film ($1240/\lambda_{onset}$). [e] Onset oxidation and reduction potentials,

respectively. [f] Estimated from the onset oxidation and reduction potentials, respectively. [g] Electronic bandgap estimated from electrochemistry.

Table S2. Calculated absorption data for the polymers of **P1**, **P2**, **P3** and **P4**.

Compound	Excited state	Transfer type	Wave length (nm)	f
P1	1	Singlet-A	751.44	0.0628
	6	Singlet-A	401.06	1.3500
	8	Singlet-A	369.69	0.1341
	9	Singlet-A	363.39	0.1600
	10	Singlet-A	348.86	0.2354
	12	Singlet-A	337.17	0.4144
	13	Singlet-A	320.07	0.1834
	17	Singlet-A	290.39	0.1171
	19	Singlet-A	286.06	0.1559
	36	Singlet-A	252.42	0.1050
P2	1	Singlet-A	791.45	0.0569
	4	Singlet-A	432.95	0.9406
	8	Singlet-A	386.01	0.6015
	9	Singlet-A	374.41	0.1396
	10	Singlet-A	360.05	0.3339
	12	Singlet-A	346.80	0.3135
	15	Singlet-A	319.74	0.2297
	21	Singlet-A	292.68	0.1258
	71	Singlet-A	237.52	0.1035
P3	1	Singlet-A	761.74	0.0636
	5	Singlet-A	408.09	0.4532
	7	Singlet-A	402.61	0.8467
	10	Singlet-A	354.65	0.2580
	11	Singlet-A	345.96	0.2395
	12	Singlet-A	340.35	0.2026
	13	Singlet-A	334.14	0.2056
	14	Singlet-A	317.41	0.1445
	19	Singlet-A	285.24	0.1966
	82	Singlet-A	5.4723	0.1762
P4	1	Singlet-A	888.24	0.0678
	5	Singlet-A	452.83	1.0884
	8	Singlet-A	371.05	0.2266
	9	Singlet-A	368.11	0.3925
	12	Singlet-A	356.10	0.1312
	13	Singlet-A	345.35	0.2121
	14	Singlet-A	329.48	0.5071
	20	Singlet-A	297.01	0.1114

Table S3. XRD data of polymer films after annealing at 80℃ in vacuum for 1 hour.

Polymer	P1	P2	P3	P4
2θ (degree)	4.00	3.46	4.08	4.04
d-spacing (Å)	22.07	25.52	21.64	21.86

6. Characterization data for key products

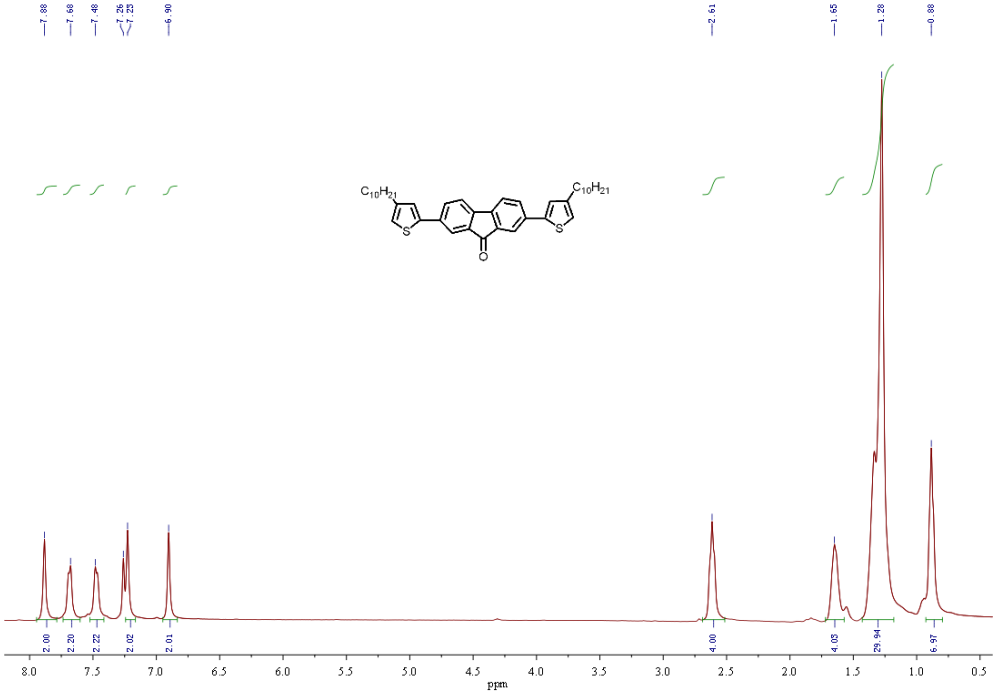

Figure S8. ^{1}H NMR (400MHz) of compound **2** in $CDCl_3$.

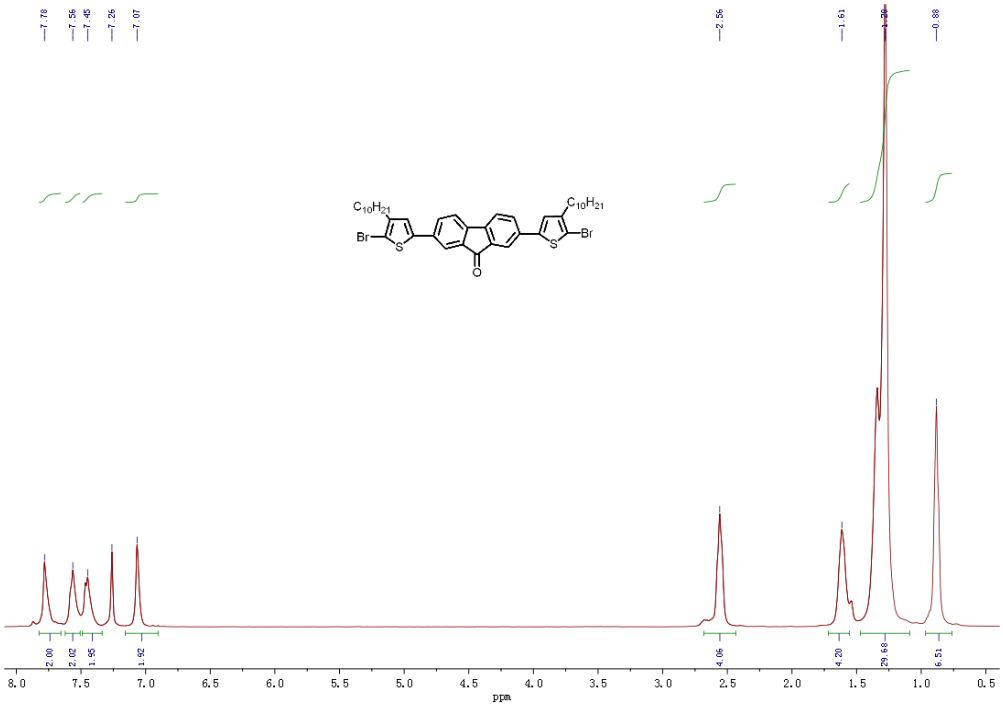

Figure S9. ^{1}H NMR (400MHz) of compound **3** in $CDCl_3$.

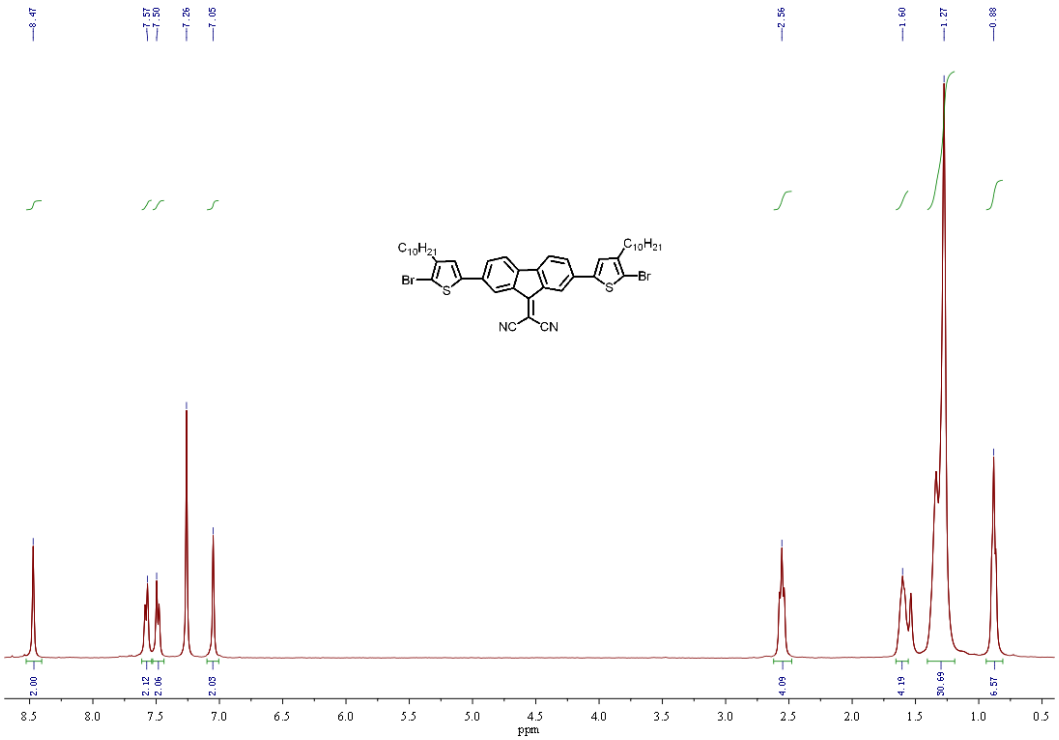

Figure S10. ^{1}H NMR (400MHz) of CN-Fluorene (compound **4**) in $CDCl_3$.

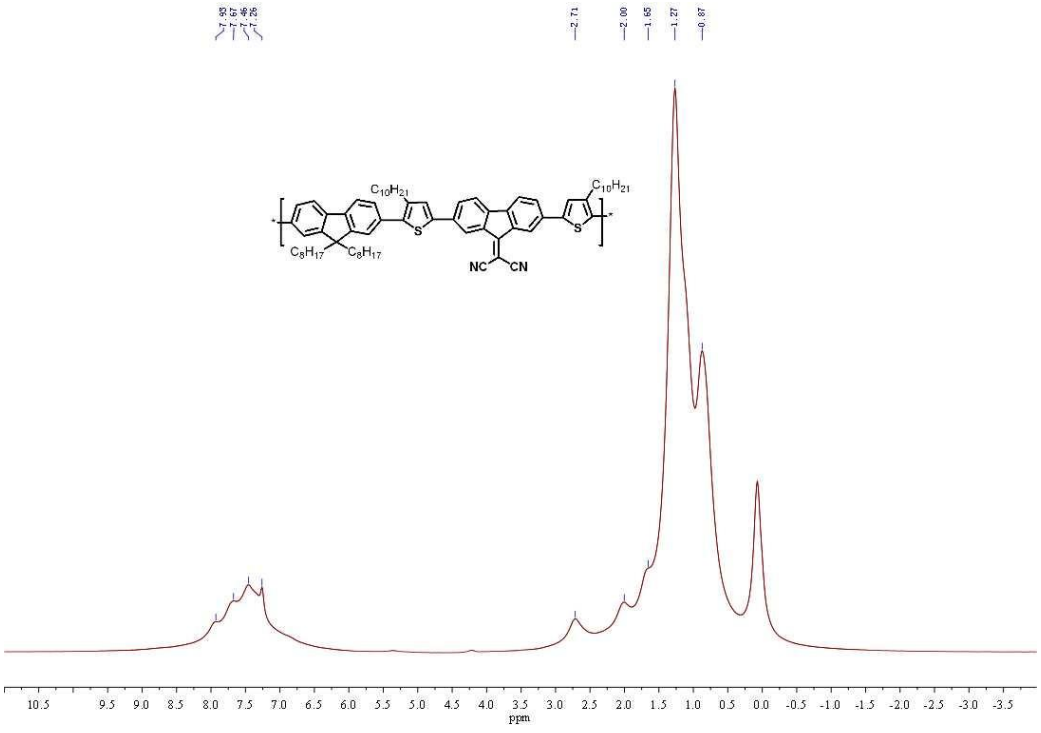

Figure S11. ^{1}H NMR (400MHz) of **P1** in $CDCl_3$.

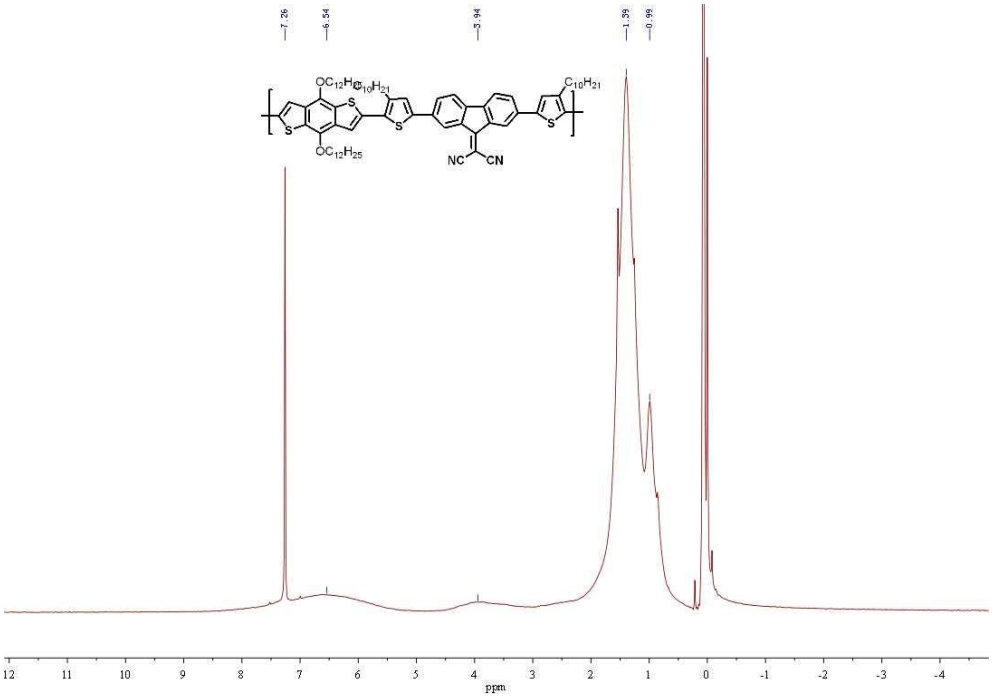

Figure S12. ^{1}H NMR (400MHz) of **P2** in $CDCl_3$.

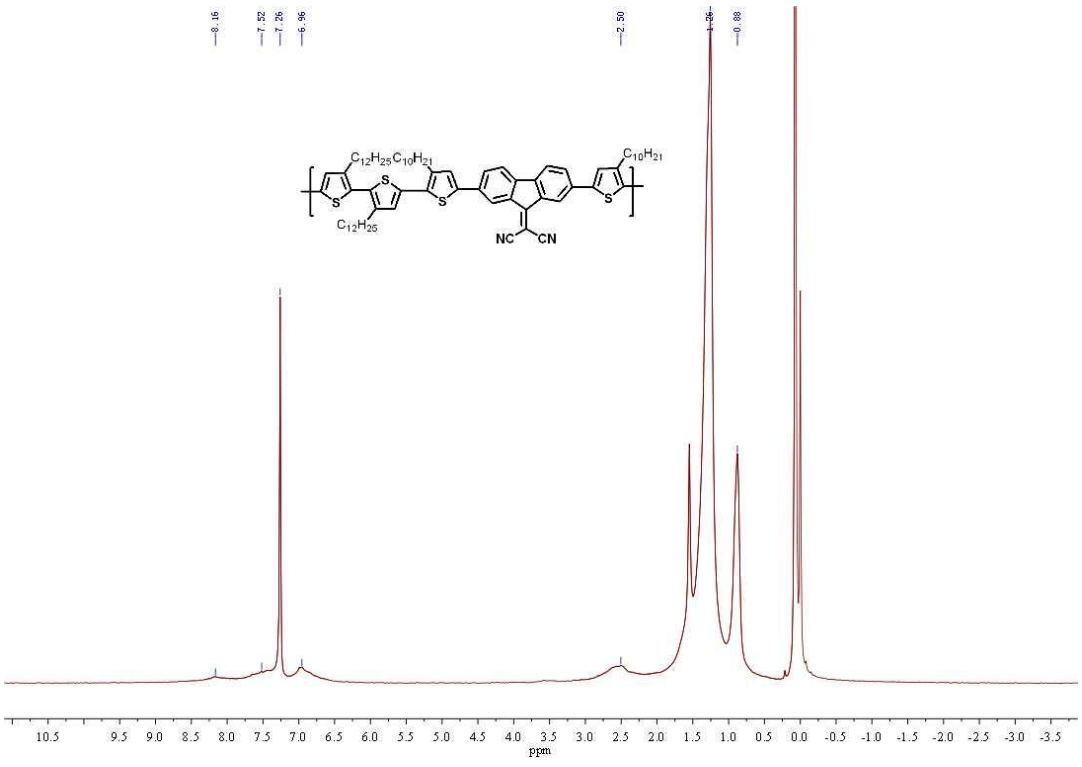

Figure S13. ^{1}H NMR (400MHz) of **P3** in $CDCl_3$.

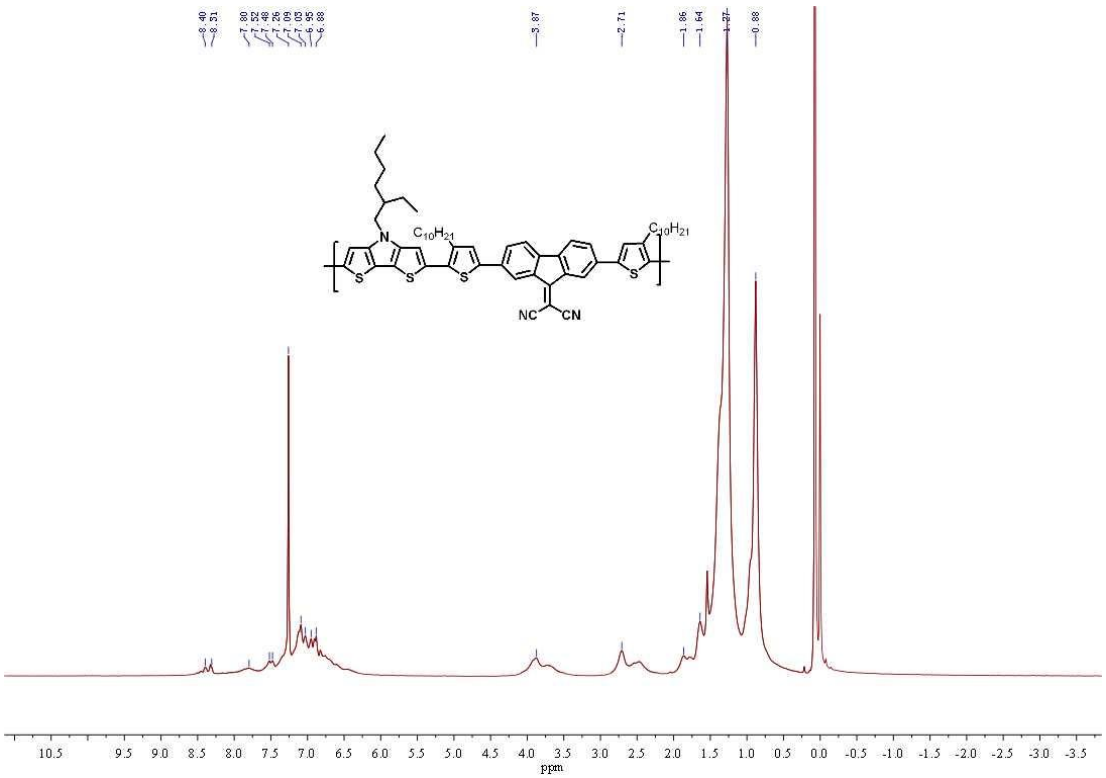

Figure S14. ^{1}H NMR (400MHz) of **P4** in $CDCl_3$.

5. References:

[1] M. J. Frisch, G. W. Trucks, H. B. Schlegel, G. E. Scuseria, M. A. Robb, J. R. Cheeseman, J. A. Montgomery Jr., T. Vreven, K. N. Kudin, J. C. Burant, J. M. Millam, S. S. Iyengar, J. Tomasi, V. Barone, B. Mennucci, M. Cossi, G. Scalmani, N. Rega, G. A. Petersson, H. Nakatsuji, M. Hada, M. Ehara, K. Toyota, R. Fukuda, J. Hasegawa, M. Ishida, T. Nakajima, Y. Honda, O. Kitao, H. Nakai, M. Klene, X. Li, J. E. Knox, H. P. Hratchian, J. B. Cross, V. Bakken, C. Adamo, J. Jaramillo, R. Gomperts, R. E. Stratmann, O. Yazyev, A. J. Austin, R. Cammi, C. Pomelli, J. W. Ochterski, P. Y. Ayala, K. Morokuma, G. A. Voth, P. Salvador, J. J. Dannenberg, V. G. Zakrzewski, S. Dapprich, A. D. Daniels, M. C. Strain, O. Farkas, D. K. Malick, A. D. Rabuck, K. Raghavachari, J. B. Foresman, J. V. Ortiz, Q. Cui, A. G. Baboul, S. Clifford, J. Cioslowski, B. B. Stefanov, G. Liu, A. Liashenko, P. Piskorz, I. Komaromi, R. L. Martin, D. J. Fox, T. Keith, M. A. Al-Laham, C. Y. Peng, A. Nanayakkara, M. Challacombe, P. M. W. Gill, B. Johnson, W. Chen, M. W. Wong, C. Gonzalez, and J. A. Pople, (Gaussian 03, Revision C.02, Gaussian, Inc., Wallingford CT, 2004).

[2] A. D. Becke, J. Chem. Phys. **98**, 5648 (1993).

[3] A. D. Becke, Phys. Rev. A **38**, 3098 (1988).

[4] C. T. Lee, W. T. Yang, and R. G. Parr, Phys. Rev. B **37**, 785 (1988).

[5] M. E. Casida, *Recent developments and applications of modern density functional theory, p 391*. (Elsevier, Amsterdam, 1996).

[6] (a) E. Ahmed, S. Subramaniyan, F. S. Kim and H. Xin, S. A. Jenekhe, *Macromolecules*, 2011, **44**, 7207. (b) X. Zhang, L. J. Richter, D. M. Delongchemp, R. J. Kline, M. R. Hammond, I. M. Culloch, M. Heeney, R. S. Ashraf, J. N. Smith, T. D. Anthopoulous, B. Schroeder, Y. H. Geerts, D. A. Fisher and M. F. Toney, *J. Am. Chem. Soc.*, 2011, **133**, 15073.